THE JOURNAL OF BIOLOGICAL CHEMISTRY VOL. 287, NO. 42, pp. 35104–35117, October 12, 2012

Neogenin Interacts with Matriptase-2 to Facilitate Hemojuvelin Cleavage*

Received for publication, March 19, 2012, and in revised form, July 28, 2012 Published, JBC Papers in Press, August 14, 2012, DOI 10.1074/jbc.M112.363937

Caroline A. Enns, Riffat Ahmed, and An-Sheng Zhang[1]

From the Department of Cell and Developmental Biology, Oregon Health and Science University, Portland, Oregon 97239

Background: Matriptase-2 regulates iron homeostasis by binding to and cleaving hemojuvelin. Neogenin interacts with hemojuvelin.
Results: Matriptase-2 forms a complex with both neogenin and hemojuvelin. Disruption of the hemojuvelin-neogenin interaction abolishes the cleavage of hemojuvelin by matriptase-2.
Conclusion: Neogenin is required for matriptase-2 cleavage of hemojuvelin.
Significance: Neogenin is involved in iron homeostasis by interacting with both matriptase-2 and hemojuvelin.

Hemojuvelin (HJV) and matriptase-2 (MT2) are co-expressed in hepatocytes, and both are essential for systemic iron homeostasis. HJV is a glycosylphosphatidylinositol-linked membrane protein that acts as a co-receptor for bone morphogenetic proteins to induce hepcidin expression. MT2 regulates the levels of membrane-bound HJV in hepatocytes by binding to and cleaving HJV into an inactive soluble form that is released from cells. HJV also interacts with neogenin, a ubiquitously expressed transmembrane protein with multiple functions. In this study, we showed that neogenin interacted with MT2 as well as with HJV and facilitated the cleavage of HJV by MT2. In contrast, neogenin was not cleaved by MT2, indicating some degree of specificity by MT2. Down-regulation of neogenin with siRNA increased the amount of MT2 and HJV on the plasma membrane, suggesting a lack of neogenin involvement in their trafficking to the cell surface. The increase in MT2 and HJV upon neogenin knockdown was likely due to the inhibition of cell surface MT2 and HJV internalization. Analysis of the Asn-linked oligosaccharides showed that MT2 cleavage of cell surface HJV was coupled to a transition from high mannose oligosaccharides to complex oligosaccharides on HJV. These results suggest that neogenin forms a ternary complex with both MT2 and HJV at the plasma membrane. The complex facilitates HJV cleavage by MT2, and release of the cleaved HJV from the cell occurs after a retrograde trafficking through the TGN/Golgi compartments.

Iron is an essential nutrient in nearly all organisms. It is also toxic when in excess. Because humans cannot control the secretion of excess iron from the body, systemic iron homeostasis is maintained by coordinately regulating the dietary iron absorption in the duodenum, iron recycling of senescent erythrocytes in macrophages, and mobilizing stored iron in the liver. Hepcidin, the key iron regulatory hormone, plays an essential role in this process. This 25-amino acid peptide is secreted predominantly by hepatocytes, and it inhibits iron efflux into the circulation by binding to and targeting ferroportin on plasma membrane for degradation. Ferroportin is the only known iron exporter. It is expressed on duodenal enterocytes, macrophages, and hepatocytes (1, 2). Lack of hepcidin causes juvenile hemochromatosis (3), a particularly severe form of iron overload disorder. In contrast, inappropriately high levels of hepcidin cause iron-deficiency anemia (4). Hepcidin expression is positively regulated by iron levels in the body, providing a negative feedback to decrease further iron uptake into the body. Recent studies identified hemojuvelin (HJV)[2] and matriptase-2 (MT2) as a pair of key regulators in iron homeostasis, but the precise mechanisms by which they function *in vivo* are unknown (5, 6).

HJV is a glycosylphosphatidylinositol-linked membrane protein (7) that is encoded by the *HFE2* gene in humans and the *Hjv* gene in mice. It is mainly expressed in hepatocytes, skeletal muscle, and heart (5). Homozygous or compound heterozygous mutations of *HFE2* in humans markedly reduce hepatic hepcidin expression and result in juvenile hemochromatosis with the clinical manifestations indistinguishable from lack of hepcidin (5, 8). Similarly, a pronounced decrease in hepcidin expression and a severe iron overload are also present in mice with a global disruption of both *Hjv* alleles (9, 10), indicating that the mutations reported in humans are lack of function mutations. Thus, HJV is a robust inducer of hepcidin expression (11).

Hepatocyte HJV acts as a co-receptor for several bone morphogenetic proteins (BMPs), which induce hepcidin expression through the BMP signaling pathway (11, 12). Expression of *Hjv* in hepatocytes of *Hjv*-null mice is able to correct the defects of iron metabolism (13). In agreement with this finding, studies in mice with tissue-specific *Hjv* knockdown demonstrate that hepatocyte-specific expression of *Hjv* is essential for hepcidin expression, whereas skeletal muscle *Hjv* is not (14, 15).

HJV levels can be regulated by MT2, a serine protease, which is predominantly expressed in hepatocytes (16, 17) and

* This work was supported, in whole or in part, by National Institutes of Health Grants DK080765 (to A. S. Z.) and DK72166 (to C. A. E.).
[1] To whom correspondence should be addressed: Dept. of Cell and Developmental Biology L215, Oregon Health and Science University, 3181 SW Sam Jackson Park Rd., Portland, OR 97239. Tel.: 503-494-5846; Fax: 503-494-4253; E-mail: zhanga@ohsu.edu.

[2] The abbreviations used are: HJV, hemojuvelin; BMP, bone morphogenetic protein; TGN, trans-Golgi network; CM, conditioned medium; MEM, minimum Eagle's medium; FCI, furin convertase inhibitor; Endo-H, endo-β-*N*-acetylglucosaminidase H; PNGase F, peptide:*N*-glycosidase F; qRT, quantitative real time; ER, endoplasmic reticulum.

encoded by the *TMPRSS6* gene in humans (denoted as *Tmprss6* in mice) (18). This type II transmembrane protease is composed of a short cytoplasmic domain, a transmembrane domain, and a large extracellular domain, which contains a membrane-proximal SEA (sea urchin sperm protein, enteropeptidase, agrin) domain, two CUB (complete protein subcomponents C1r/C1s motif, urchin embryonic growth factor, and BMP1) domains, three low density lipoprotein receptor class A domains, a predicted activation domain, and a C-terminal catalytic domain (Fig. 1*A*) (19). The MT2 catalytic domain is responsible for the cleavage of HJV at arginine 288, releasing a 36-kDa soluble form of HJV that is incapable of binding BMPs (20) making MT2 a suppressor of hepcidin expression (21). Mutations of *TMPRSS6* result in increased hepcidin expression, which leads to iron-refractory, iron deficiency anemia (6). Similar phenotypes are also reported in mouse models either with knockdown of both *Tmprss6* alleles or with a mutant *Tmprss6* that lacks the catalytic domain (*mask* mice) (18, 22). The stem region of the MT2 ectodomain (Fig. 1*A*) binds to HJV (21). Interestingly, mice with the disruption of both *Hjv* and *Tmprss6* genes display a phenotype that is indistinguishable from *Hjv*-null mice. The phenotypes of high hepcidin expression and iron deficiency detected in *Tmprss6*-null mice are totally blunted (23, 24). These observations support the idea that both MT2 and HJV regulate hepcidin expression through the same pathway and that HJV lies downstream of MT2.

In addition to MT2, HJV can also be cleaved by the ubiquitously expressed furin (25–27). The furin cleavage site of HJV is distinct from that of MT2 (20). Furin cleavage of HJV generates a 40-kDa fragment, and it is neogenin-dependent in HepG2 cells, a human hepatoma cell line (28, 29). The role that neogenin plays in the cleavage of HJV is controversial. Another group reported that neogenin suppresses HJV secretion from cultured mouse muscle and transiently transfected HEK293 cells (30).

Neogenin is a ubiquitously expressed membrane protein composed of a large extracellular domain that contains four immunoglobulin-like domains and six fibronectin III (FNIII) domains (Fig. 1*B*) (31). It was originally identified as a receptor for repulsive guidance molecule-a (RGMa), which belongs to the same family of proteins as HJV (32). HJV also binds neogenin (7, 33). *In vitro* analysis of neogenin fragments demonstrated that the FNIII 5–6 domains bind HJV with a subnanomolar binding affinity (34). Whether neogenin is involved in the MT2 cleavage of HJV is unknown, and it is the subject of this study.

In this study, we demonstrate that neogenin forms a complex with both MT2 and HJV. Down-regulation of neogenin with siRNA increased the amount of MT2 on the plasma membrane and blocked MT2 cleavage of HJV. Further analysis suggests that MT2 cleavage of HJV occurs either at the cell surface or during a retrograde trafficking to the TGN/Golgi compartment in a neogenin-dependent manner.

EXPERIMENTAL PROCEDURES

Cell Culture and Transfection—Both HepG2 and human embryonic kidney 293 (HEK293) cells were purchased from the ATCC (Manassas, VA) and maintained in MEM, 10% FCS, 1 mM pyruvate, 1× nonessential amino acids or DMEM, 10% FCS, 1 mM pyruvate, respectively. HepG2 cells stably transfected with pcDNA3 empty vector (HepG2-Ctrl), HJV (HepG2-HJV) or MT2 (HepG2-MT2), and HEK293 cells stably transfected with pcDNA3 empty vector (HEK293-Ctrl), pcDNA3-HJV (HEK293-HJV), or stably co-transfected with both HJV and neogenin (HEK293-HJV/Neo) were generated previously (20). The stably transfected cells were maintained in complete medium with 800 μg/ml G418. HepG2 cells stably expressing full-length neogenin (HepG2-Neo) were generated using the same strategy as described previously (20). HEK293 cells stably expressing full-length neogenin (HEK293-Neo) or truncated neogenin with no cytoplasmic domain (HEK293-NeoΔCD) (Fig. 1*B*) were established by transfecting pcDNA3-neogenin or pcDNA3-NeoΔCD plasmid DNA using Lipofectamine 2000 (Invitrogen), respectively. pcDNA3-NeoΔCD construct was made by adding a stop codon after glutamine 1135, which is localized at the 9th amino acid after the predicted transmembrane domain of neogenin cDNA sequence, using the QuikChange site-directed mutagenesis kit (Stratagene, Santa Clara, CA) and the following primers: 5′-CGTCGTACCACCTCTCACTAGAAAAAGAAACGAGCTG-3′ and 5′-CAGCTCGTTTCTTTTTCTAGTGAGAGGTGGTACGACG-3′. PolyJet (SignaGen Laboratories) and Lipofectamine 2000 transfection reagent were used to transiently transfect HepG2 and HEK293 cells, respectively.

Soluble Neogenin—Soluble forms of neogenin, including the entire extracellular domain (Neo/Ecto), neogenin fibronectin III domains 1–6 (FNIII 1–6), and neogenin FNIII 5–6 (Fig. 1*B*), were generated using baculovirus, as described previously (34), and kindly provided by Drs. Pamela Bjorkman and Fan Yang, California Institute of Technology. They were added directly into the culture medium of HEK293-HJV and HepG2-HJV cells at the indicated concentration as described in the figure legends to determine the effect on the secretion of MT2-cleaved HJV or MT2 degradation.

Knockdown of Endogenous Neogenin—Neogenin siRNA (Dharmacon) was used to knock down the endogenous neogenin in HepG2-HJV cells or HepG2-MT2 cells, as described previously (35), using RNAiMAX (Invitrogen) for transfection. The negative control siRNA was the same as described previously (35). Cells were transfected twice on days 1 and 3 to maximize the efficacy of the knockdown. For HepG2-HJV cells, both cell lysate and the conditioned medium (CM) were collected for analysis by Western blot 72 h after the second transfection. For HepG2-MT2 cells, cell surface proteins were subjected to biotinylation at 4 °C about 72 h after the second transfection to determine the effects of neogenin on MT2 expression at the plasma membrane. Alternatively, about 66 h after the second transfection, HepG2-MT2 cells were subjected to incubation with 100 μg/ml cycloheximide in complete medium for the time intervals as described in the figure legend, to determine the effects of neogenin depletion on MT2 degradation.

Neogenin Release—HEK293 and HepG2 cells expressing neogenin, HJV, or MT2 were incubated in MEM, 1% FCS in the presence of furin convertase inhibitor (FCI; Enzo Life Sciences), leupeptin (Sigma), or TAPI-2 (Calbiochem) at the concentrations indicated in the figure legends. After incubation at 37 °C

in a CO_2 incubator for the time intervals indicated in the figure legends, conditioned medium and cell lysates were collected for immunodetection of neogenin, HJV, and MT2.

Immunoprecipitation—Cells were metabolically labeled with [^{35}S]Met/Cys (PerkinElmer Life Sciences) at 100 μCi/ml in MEM (without Met/Cys), 2% FCS for 3 h at 37 °C. After washing with cold PBS on ice, cell lysates were prepared using NET-Triton buffer (150 mM NaCl, 5 mM EDTA, 10 mM Tris, pH 7.4, and 1% Triton X-100) with 1× protease inhibitors mixture (Roche Diagnostics). Immunoprecipitation was performed as described previously (36) using protein A-agarose beads (Invitrogen), rabbit anti-HJV 18745 antibody (generated against residues 1–401 of HJV), rabbit anti-neogenin 21567 antibody (generated against the neogenin ectodomain FNIII 1–6), or rabbit anti-MT2 23144 IgG (generated against the stem region of MT2 ectodomain). Immunoprecipitated proteins bound to protein A-agarose beads were washed, eluted, and separated by SDS-PAGE. Images were obtained by exposure to x-ray film.

Biotinylation of Cell Surface Proteins—HepG2-MT2 or HepG2-HJV cells in a 6-well plate at ~80% confluence were biotinylated with 0.25 mg/ml Sulfo-NHS-Biotin (Thermo Fisher Scientific) at 4 °C for 30 min. After the reaction was terminated, cells were immediately solubilized in NET-Triton, 1× protease inhibitors mixture (Roche Diagnostics). Biotinylated proteins were isolated using streptavidin-agarose beads (Thermo Fisher Scientific). Bound proteins were eluted with NET-Triton, 1% β-mercaptoethanol, 0.5% SDS and subjected to digestion with Endo-H or PNGase F, followed by immunodetection of MT2, HJV, TfR1, Na^+/K^+-ATPase α1, and β-actin.

Analysis of HJV Secretion—Cell surface HJV in HepG2-HJV cells was biotinylated at 4 °C as described above. Cells were then incubated in complete medium at 37 °C for 4 h. The total biotinylated cell surface proteins before incubation at 37 °C and the biotinylated proteins collected in the CM/pulldown after incubation at 37 °C were isolated using streptavidin-agarose beads. The eluates were subjected to Endo-H and PNGase F digestion, followed by immunodetection of HJV.

Endo-H and PNGase F Digestion—Endo-H and PNGase F (New England Biolabs) were used to analyze the Asn-linked oligosaccharides on MT2, neogenin, and HJV protein in cell lysate and streptavidin bead eluate or secreted HJV in conditioned medium. Briefly, samples were incubated with Endo-H or PNGase F for 4 h at 37 °C according to manufacturer's instruction. The digested proteins were subjected to Western blot analysis as described under "Immunodetection."

Liver Membrane Preparation—Snap-frozen liver tissues from wild type, *Tmprss6-null* mice (−/−), and neogenin-mutant mice were crushed in liquid nitrogen, followed by homogenization using a metal Dounce homogenizer in ice-cold HEM lysis buffer (20 mM Hepes, pH 7.4, 1 mM EDTA, and 300 mM mannitol) containing protease inhibitors mixture. After removing the nuclei and insoluble debris by centrifugation at 10,000 × *g* for 10 min, the supernatant was subjected to a high speed centrifugation at 100,000 × *g* for 60 min at 4 °C to pellet membranes. Membrane pellets were solubilized in NET-Triton, 1× protease inhibitors mixture. The membrane extract proteins (250 μg) were separated using SDS-PAGE (11%) under reducing conditions, followed by immunodetection of MT2, neogenin, and β-actin.

Liver tissues from 8-week-old male wild type and *Tmprss6*$^{-/-}$ mice were kindly provided by Dr. Thomas Bartnikas and Dr. Mark Fleming, Harvard University. Heterozygous neogenin (*Neo*) mutant mice on a B6.129 background were purchased from Mutant Mouse Regional Research Center, University of Missouri. This mouse colony is maintained at Oregon Health and Science University DCM. Wild type, *Neo*$^{+/-}$, and *Neo*$^{-/-}$ male littermates at about 24 days were obtained by cross-breeding the heterozygous mice. Neogenin mutation was confirmed by genotyping by PCR. All procedures for animal uses were approved by Oregon Health and Science University DCM.

Quantitative Real Time RT-PCR (qRT-PCR)— qRT-PCR was used to analyze *Tmprss6* mRNA levels in whole liver tissues of neogenin mutant mice and *TMPRSS6* mRNA levels in HepG2 and HepG2-MT2 cells with and without neogenin knockdown. The procedures for total RNA isolation and cDNA preparation were described previously (37). qRT-PCR analysis was performed as reported previously (20). Primers used are 5′-ctgtgcagcgaggtctatcg-3′ (human *TMPRSS6*, forward), and 5′-agtcaccctgacaggcatcct-3′ (human *TMPRSS6*, reverse); 5′-aggtcatcaccattggcaatg-3′ (human β-actin, forward), and 5′-gtcacacttcatgatggagttgaag-3′ (human β-actin, reverse). The sequences for mouse *Tmprss6* and mouse β-actin are the same as reported previously (13, 38). All primers were verified for linearity of amplification. The results for each gene of interest are expressed as the amount of mRNA relative to β-actin.

Immunodetection—Cell lysates, conditioned medium, or streptavidin eluates were separated by SDS-PAGE under reducing conditions, followed by transfer onto a nitrocellulose membrane. Membranes were probed with affinity-purified rabbit anti-HJV 18745 antibody (0.22 μg/ml), rabbit anti-neogenin 21567 antibody (1:10,000), rabbit anti-MT2 23144 IgG, mouse anti-TfR1 (1:10,000; Zymed Laboratories Inc.), mouse anti-Na^+/K^+-ATPase α1 (1:500; Santa Cruz Biotechnology), or mouse anti-β-actin antibody (1:10,000; Chemicon International), followed by immunodetection using a corresponding horseradish peroxidase (HRP)-conjugated secondary antibody (Chemicon International) and chemiluminescence (Super Signal, Pierce). Alternatively, MT2 was detected using an Alexa Fluor 680 goat anti-rabbit secondary antibody (1:10,000; Invitrogen) and visualized using an Odyssey Infrared Imaging System (Licor). In all the immunodetections, membranes were always probed with one single antibody each time. Most of the membranes were probed sequentially with multiple antibodies without stripping to show the changes of different proteins in a single image. We always probed the membrane with anti-MT2 antibody first to detect the potential cleavage products in the cell lysates.

RESULTS

Neogenin Is Required for MT2 Cleavage of HJV—MT2 suppresses hepcidin expression by cleaving the glycosylphosphatidylinositol-linked membrane HJV into an inactive 36-kDa fragment that is released from hepatocytes (21, 39). Proteolytic release of HJV from HepG2 cells that stably express transfected

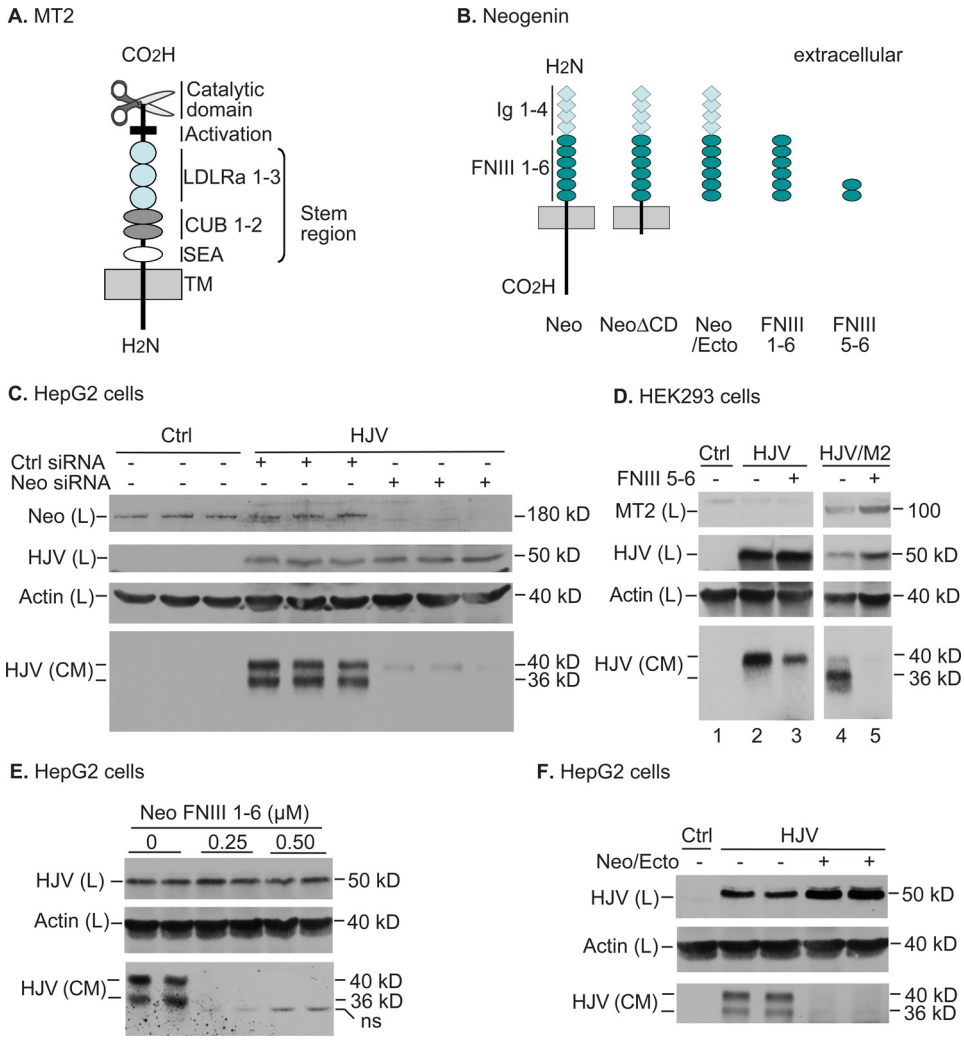

FIGURE 1. **Neogenin is required for MT2 cleavage of HJV.** *A,* diagram of the MT2 protein. MT-2 is a type II transmembrane protein that has a short cytoplasmic domain, a transmembrane domain, and a large extracellular domain. The extracellular domain contains a membrane-proximal *SEA* (sea urchin sperm protein, enteropeptidase, agrin) domain, two *CUB* (complete protein subcomponents C1r/C1s motif, urchin embryonic growth factor, and BMP1) domains, three *LDLRa* (low density lipoprotein receptor class A) domains, a predicted activation domain, and a C-terminal catalytic domain. *B,* diagram of different forms of neogenin used in this study. Full-length neogenin (*Neo*) is a type I transmembrane protein with a large extracellular domain that contains four immunoglobulin-like domains (*Ig 1–4*) and six fibronectin III domains (*FNIII 1–6*). *NeoΔCD* is a truncated form of neogenin lacking the cytoplasmic domain. Its cDNA construct was generated by adding a stop codon immediately after glutamine 1135, the 9th amino acid after the predicted transmembrane domain of the neogenin sequence. *Neo/Ecto* is a soluble form of neogenin that lacks both the cytoplasmic domain and transmembrane domains. *FNIII 1–6* is a soluble form of neogenin that contains FNIII 1–6 domains. *FNIII 5–6* is a soluble form of neogenin that contains FNIII 5–6 domains. *C,* knockdown of endogenous neogenin blocks the secretion of MT2-cleaved HJV in HepG2-HJV cells. HepG2-HJV cells (*HJV*) were transfected with a control (*Ctrl*) or neogenin siRNA twice on day 1 and day 3. At 72 h after the second transfection, neogenin (*Neo*), HJV, and β-actin in total cell lysate (*L*) and HJV in 15% CM were immunodetected using the corresponding antibodies. HepG2-Ctrl cells (*Ctrl*) were included as a negative control for HJV. *D,* neogenin FNIII 5–6 blocks the release of MT2-cleaved HJV in HEK293 cells. HEK293-HJV cells were transiently transfected with either MT2 cDNA (HJV/MT2) or pcDNA3 empty vector, followed by incubation in the absence or presence of 40 nM FNIII 5–6 in DMEM, 5% FCS for about 16 h. MT2, HJV, and β-actin in total cell lysate (*L*) and HJV in 15% CM were immunodetected. HEK293-Ctrl cells (*Ctrl*) are included as a control for HJV. All images are from a single gel. *E,* neogenin FNIII 1–6 blocks HJV release from HepG2 cells. HepG2-HJV cells were incubated in the absence or presence of 0.25 or 0.5 μM neogenin FNIII 1–6 in MEM, 5% FCS for about 16 h. HJV and β-actin in total cell lysate (*L*) and HJV in 15% CM were immunodetected. *F,* Neo/Ecto blocks HJV release from HepG2 cells. The experiments were performed as described in *E* except that 0.5 μM Neo/Ecto was added. All experiments were repeated at least three times with consistent results.

HJV (HepG2-HJV) constitutes the major pathway of HJV turnover (36). HepG2 cells endogenously express MT2, furin, and neogenin (20). Down-regulation of endogenous neogenin using siRNA in HepG2-HJV cells blocks the secretion of two major forms of soluble HJV that migrate at 36 kDa (MT2 cleavage product) and 40 kDa (furin cleavage product) in SDS-PAGE, respectively (Fig. 1*C*, *CM*). The relative amounts of HJV in the conditioned medium represented the accumulation during 72 h of culture after the second siRNA knockdown. Because HJV is overexpressed in these cells, the endogenous levels of MT2 and furin were not sufficient to substantially decrease cellular levels of HJV (Fig. 1*C*). No cleavage product was detectable in the cell extracts by Western blot indicating that cleavage occurs either at the cell surface or that the release occurs shortly after cleavage (data not shown). HepG2 cells that were stably transfected with pcDNA3 empty vector (HepG2-Ctrl) were included as a negative control for HJV. These results along with the previous observations, which showed that furin cleavage of HJV is not required for M2 cleavage (20), indicate that neogenin is required for the cleavage of HJV by both MT2 and furin.

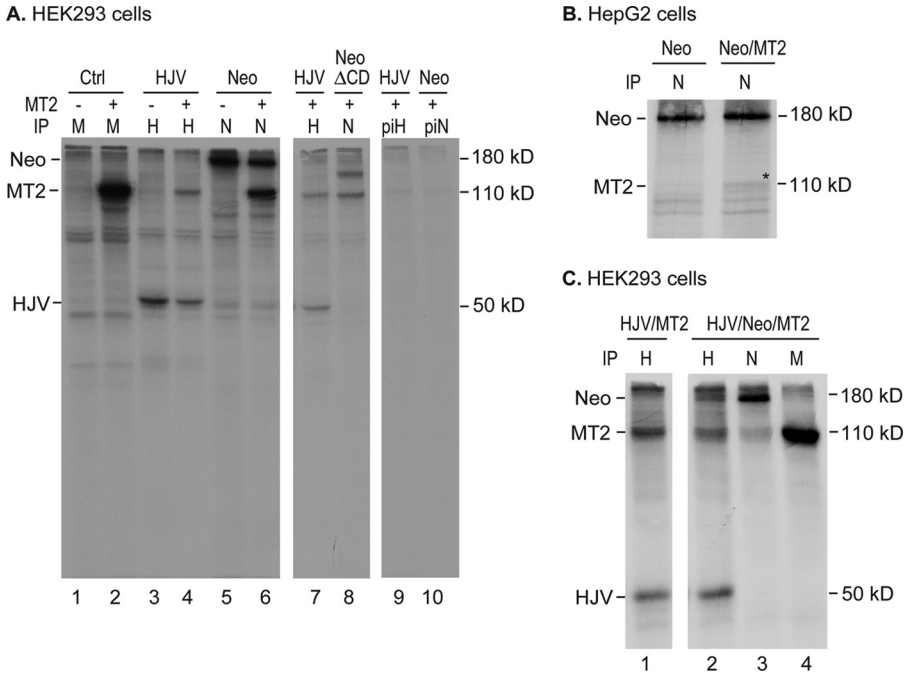

FIGURE 2. **Neogenin interacts with both HJV and MT2.** *A,* MT2 interacts with neogenin in HEK293 cells. HEK293 cells expressing MT2 alone, HJV alone, neogenin (*Neo*) alone, MT2/HJV, MT2/Neo, or MT2/NeoΔCD were metabolically labeled with 100 μCi of [^{35}S]Met/Cys/ml for 3 h. Immunoprecipitations (*IP*) were performed using rabbit anti-HJV antibody 18745 (*H*; generated against residues 1–401 of HJV), rabbit anti-neogenin 21567 antibody (*N*; generated using the neogenin FNIII 1–6 domains), or rabbit anti-MT2 antibody 23144 (*M*; generated against the stem region of MT2). Immunoprecipitated proteins were separated by SDS-PAGE, followed by soaking of the gel in Amplify (GE Healthcare) and drying of the gels prior to exposure to x-ray film. The preimmune serum for HJV (*piH*) and neogenin (*piN*) were included as negative controls. All images are from a single gel. *B,* MT2 interacts with neogenin in HepG2 cells. HepG2 cells stably transfected with neogenin (*Neo*) were transiently transfected with either pcDNA3 or MT2 cDNA (*MT2*), followed by a metabolic labeling with 100 μCi of [^{35}S]Met/Cys/ml, as described in *A,* and immunoprecipitation using anti-neogenin antibody. * indicates the MT2 band. *C,* HJV interacts with both neogenin and MT2. HEK293 cells expressing HJV/MT2 or HJV/Neo/MT2 were metabolically labeled and immunoprecipitated as described in *A* using anti-HJV (*H*), neogenin (*N*), or MT2 (*M*) antibody. Images are from a single gel. All experiments were repeated at least three times with similar results.

Neogenin could have an indirect effect on the cleavage of HJV. To further test whether disruption of the interaction between neogenin and HJV inhibits HJV cleavage, we used soluble fragments of neogenin to compete with the binding of HJV to the endogenous neogenin (Fig. 1*B*). HJV binds to the FNIII 5–6 domains of neogenin (34). We examined three forms of soluble neogenin, FNIII 5–6 (~30 kDa), FNIII 1–6 (~90 kDa), and Neo/Ecto (~150 kDa), for their ability to interfere with the neogenin-facilitated cleavage of HJV. They all bind HJV *in vitro* with the binding affinity at about 0.22, 560, and 2,100 nM (34). All three forms of soluble neogenin are expected to act as decoys that compete with the binding of HJV to endogenously expressed neogenin at the cell surface. HEK293-control cells (transfected with an empty vector), HEK293-HJV cells (transfected with HJV), and HEK293-HJV/MT2 cells (transfected with HJV and MT2) were used. HEK293 cells endogenously express both neogenin and furin. Addition of FNIII 5–6 domains of neogenin (40 nM) into the culture medium of HEK293-HJV cells reduced the cleavage of HJV by furin (Fig. 1*D*, *lane 2 versus lane 3* in *CM*). When HEK293-HJV/MT2 cells were incubated with FNIII 5–6 domains of neogenin, it abolished the release of MT2-cleaved HJV (Fig. 1*D, lane 4 versus lane 5* in *CM*). Expression of MT2 significantly reduces HJV levels in the cells when compared with HEK293-HJV (Fig. 1*D, top panel, lanes 4* and *5 versus lanes 2* and *3*), consistent with the previous observations by Silvestri *et al.* (21).

Similarly, the release of cleaved HJV products by MT2 as well as by furin in HepG2-HJV cells was also blocked by addition of FNIII 1–6 domains and Neo/Ecto to the culture medium (Fig. 1, *E* and *F*). Interestingly, inhibition of HJV secretion by Neo/Ecto, rather than FNIII 1–6, resulted in an increase in cellular HJV (Fig. 1*F*). We do not have an obvious explanation for this observation. Collectively, these observations suggest that HJV cleavage by MT2 as well as by furin requires the association of HJV with full-length neogenin at the cell surface and that soluble neogenin fragments compete with this process.

MT2 Interacts with Neogenin—To determine how neogenin facilitates the MT2 cleavage of HJV, we tested whether neogenin directly interacts with MT2 and/or HJV to form a ternary complex. HEK293 cells were used as a model for this analysis, because they are easily transfected and thus are amenable to study protein interactions. HEK293 cells expressing different combinations of HJV, MT2, and neogenin were metabolically labeled with [^{35}S]Met/Cys for 3 h, followed by immunoprecipitation with anti-HJV (against residues 1–401 of HJV), anti-neogenin (generated against the neogenin ectodomain FNIII 1–6), or anti-MT2 (generated against the stem region of MT2 ectodomain) antibody. Because all three proteins undergo a rapid turnover within the cells with the half-life at about 1, 1.5, and 2.5 h for HJV, neogenin, and MT2, respectively (17, 36, 40), this time point would allow detection of the interactions under steady-state conditions. As expected, we first confirmed the previous observation that HJV interacts with MT2 (Fig. 2*A*, *lanes 4* and *7*) (21). MT2 co-immunoprecipitated with either full-length neogenin or a truncated neogenin lacking the cytoplasmic domain (NeoΔCD) (Fig. 2*A*, *lanes 6* and *8*), indicating

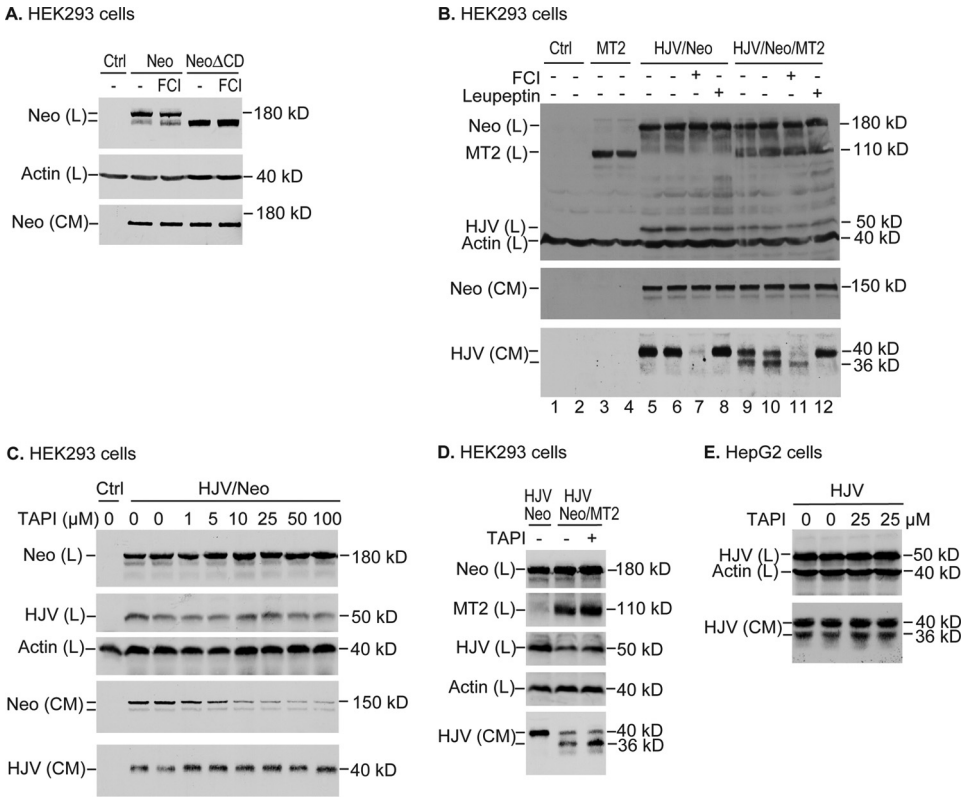

FIGURE 3. **MT2 does not cleave neogenin.** *A,* neogenin undergoes an active secretion from HEK293 cells. HEK293 cells stably transfected with pcDNA3 empty vector (*Ctrl*), full-length neogenin cDNA (*Neo*), or NeoΔCD cDNA were incubated in DMEM, 1% FCS with or without 5 μM FCI for 16 h. Neogenin (*Neo*) and β-actin in total cell lysate (*L*) and neogenin in 15% of CM were immunodetected using the corresponding antibodies. *B,* MT2 does not cleave neogenin in HEK293 cells. HEK293-Ctrl or -HJV/Neo cells were transiently transfected with MT2 cDNA or pcDNA3 empty vector. At 48 h post-transfection, medium was changed to DMEM, 1% FCS containing 5 μM FCI or 100 μM leupeptin. After 16 h of incubation, neogenin (*Neo*), MT2, HJV, and β-actin in total cell lysate (*L*) and neogenin and HJV in 15% of CM were immunodetected using the corresponding antibodies. The *top image* was obtained by a sequential probing with anti-MT2, HJV, neogenin, and β-actin antibodies. One antibody was applied each time. The membrane was not stripped before the following antibody was applied. *C,* TAPI-2 inhibits the neogenin release in HEK293 cells. HEK293-HJV/Neo cells in 12-well plates were incubated in DMEM, 1% FCS with 0, 1, 5, 10, 25, 50, or 100 μM TAPI-2 (*TAPI*) for 16 h. Neogenin, HJV, and β-actin in total cell lysate (*L*) and neogenin and HJV in 15% of CM were immunodetected using the corresponding antibodies. *D,* TAPI-2 does not affect MT2 cleavage of HJV in HEK293 cells. HEK293-HJV/Neo cells were transiently transfected with MT2 cDNA. At 48 h post-transfection, medium was changed to DMEM, 1% FCS with or without 25 μM TAPI-2 (*TAPI*). After 16 h of incubation, neogenin, MT2, HJV, and β-actin in total cell lysate (*L*), and HJV in 15% of CM were immunodetected using the corresponding antibodies. *E,* TAPI-2 does not affect HJV release from HepG2 cells. HepG2-HJV cells were incubated in MEM, 1% FCS with 0, 25, or 50 μM of TAPI-2 (*TAPI*). After 16 h of incubation, HJV and β-actin in total cell lysate (*L*) and HJV in 15% of CM were immunodetected using the corresponding antibodies. All experiments were repeated for at least three times with consistent results.

that the cytoplasmic domain of neogenin is not necessary for their interaction. Co-immunoprecipitation of MT2 with neogenin (Fig. 2*A*, *lane 6 versus lane 5* and *lane 8 versus lane 7*) indicates that MT2 interacts directly with neogenin, because HEK293 cells do not endogenously express HJV. No additional bands distinct from the controls (Fig. 2*A*) were noticed in the images after a longer exposure (data not shown) indicating that MT2, neogenin, and HJV were the major components of the complex. Consistent with these results, we also detected a co-immunoprecipitation of MT2 with neogenin in HepG2-Neo/MT2 (transfected with both neogenin and MT2) when compared with HepG2-Neo cells (transfected with neogenin alone) (Fig. 2*B*).

HJV Co-precipitates Both Neogenin and MT2—Previous studies demonstrated that neogenin interacts with HJV (7, 33, 34). We wanted to determine whether HJV, MT2, and neogenin could form a ternary complex. HEK293 cells that stably express exogenous HJV and neogenin (HEK293-HJV/Neo) were transiently transfected with MT2, followed by a metabolic labeling with [^{35}S]Met/Cys. As shown in Fig. 2*C*, anti-HJV antibody was able to pull down all three proteins (*lane 2*). Anti-MT2 antibody could bring down MT2 itself, and was included as a control for MT2 band (Fig. 2*C*, *lane 4*). Anti-neogenin antibody could pull down both neogenin and MT2 but not HJV (Fig. 2*C*, *lane 3*). The lack of detectable HJV in the immunoprecipitate might be due to a competition between the anti-neogenin antibody with HJV for binding to neogenin. The MT2 antibody made against the stem region was unable to pull down either HJV or neogenin (Fig. 2*C*, *lane 4*) consistent with the finding that MT2 interacts with HJV through its stem region (21). Our results indirectly suggest that neogenin, HJV, and MT2 could form a complex in the cells.

MT2 Does Not Cleave Neogenin—During the course of our experiments, we found a cleaved form of neogenin in the conditioned media of cells. The major M2-mediated cleavage site of HJV has been mapped to arginine 288 (20), consistent with its ability to cleave substrates immediately after an arginine residue (16). Neogenin extracellular domain possesses multiple arginine residues. We tested whether the MT2-neogenin interaction could lead to the cleavage of neogenin. First, we ruled out the possibility that a subtilisin family of proteases, like furin, could cleave neogenin by using FCI (Fig.

3*A*). Because the size of NeoΔCD in the cell extract is close to that of secreted neogenin, the cleavage site in neogenin is predicted to be at a site of extracellular domain that is adjacent to the transmembrane domain.

Transient introduction of MT2 into HEK293-HJV/Neo did not alter the amount of neogenin shed into the medium but was able to shift about half of the soluble HJV from 40 to 36 kDa (Fig. 3*B*, *lanes 5* and *6 versus lanes 9* and *10*), which is the product of MT2 cleavage (20). The lack of complete cleavage by MT2 might be due to only a portion of cells being transfected. Similar to our previous observations (20), FCI could block the release of 40-kDa soluble HJV (Fig. 3*B, lane 7 versus lanes 5* and *6*), and leupeptin blocked the release of MT2 cleavage of HJV (Fig. 3*B, lane 12 versus lanes 9* and *10*). However, neither affected the release of neogenin.

Okamura *et al.* (41) recently reported the cleavage of the extracellular domain of neogenin by the tumor necrosis factor α-converting enzyme in the transfected HEK293 cells. The cleavage product migrates at ~150 kDa in SDS-PAGE. A similar size of soluble neogenin was readily detectable in the conditioned medium of HEK293 cells transfected with either full-length neogenin or truncated neogenin (NeoΔCD) cDNA (Fig. 3*A*). In addition, the secretion of neogenin from HEK293-HJV/Neo cells was inhibited by TAPI-2, a specific tumor necrosis factor α-converting enzyme inhibitor, in a dose-dependent manner (Fig. 3*C*). This is in agreement with the observation by Okamura *et al.* (41). Conversely, TAPI-2 exhibits no evident inhibitory effect on HJV cleavage in both HEK293-HJV/Neo/MT2 cells (Fig. 3*D*) and HepG2-HJV cells (Fig. 3*E*). Interestingly, TAPI-2 mildly increased the secretion of furin-cleaved HJV in HEK293 cells (Fig. 3*C*, *lower panel*) and the MT2-cleaved HJV (Fig. 3*D*, *lower panel*), consistent with the finding that shed neogenin inhibits furin and MT2 cleavage of HJV (Fig. 1, *D–F*). Collectively, neither MT2 nor furin is able to cleave neogenin in the cells. Thus despite the interaction of MT2 with neogenin, it fails to cleave neogenin. These results indicate that MT2 is not promiscuous in its cleavage of neighboring proteins.

Lack of Neogenin Involvement in the Trafficking of MT2 to the Cell Surface—MT2 is predicted to cleave HJV at the cell surface (19, 21). We previously showed that neogenin is not required for HJV expression on the plasma membrane by flow cytometry (28). Because neogenin binds to MT2, it might act as a chaperone to facilitate the trafficking of MT2 from the ER to the plasma membrane. If this were the case, depletion of neogenin in the cells would decrease the amount of MT2 on the plasma membrane, thereby decreasing the cleavage of HJV. To test this possibility, endogenous neogenin in HepG2 cells stably expressing the transfected MT2 (HepG2-MT2) was depleted using specific siRNA. Cell surface proteins were biotinylated at 4 °C, and the biotinylated proteins were pulled down using streptavidin beads, followed by immunodetection of MT2 in the eluates. Down-regulation of endogenous neogenin resulted in the accumulation of cell surface MT2 by about 3-fold (Fig. 4, *A* and *B*). Similarly, approximately a 2-fold increase in MT2 was also detected in whole cell extracts. As a negative control, no significant change in transferrin receptor 1 (TfR1) was detected either at the cell surface or in cell lysates upon neogenin knockdown (Fig. 4*A*). These results indicate that MT2 trafficking to the plasma membrane is independent of neogenin. Rather, neogenin may facilitate MT2 turnover.

To gain more insight into the role of neogenin in MT2 turnover *in vivo*, we immunodetected the MT2 levels in the liver membrane preparations of neogenin mutant mice. This strain of mice was generated by insertion of a secretory gene-trap vector into intron 7 of the neogenin gene (42, 43). Homozygous mutant mice ($Neo^{-/-}$) have an approximate 90% reduction in neogenin protein in the liver and exhibit iron overload, low levels of hepcidin, and reduced BMP signaling (44). Consistent with the results for HepG2-MT2 cells, decreased neogenin correlates with a mild increase in MT2 in both heterozygous and homozygous mutant mice (Fig. 4*C*). Liver tissue from $Tmprss6^{-/-}$ mice was included as a negative control to show the specificity of anti-MT2 antibody. We also examined the effects of increased MT2 expression on the levels of endogenously expressed neogenin in HepG2-MT2 cells. A mild decrease was detected (Fig. 4*D*). Collectively, these results along with the observations that neogenin acts after HJV traffics to the plasma membrane in our previous studies (29) and that neogenin is necessary for MT2-induced cleavage in this study suggest that, in the absence of neogenin, expression of both HJV and MT2 at the cell surface is not enough to elicit the MT2 cleavage of HJV.

Neogenin Facilitates MT2 Protein Degradation—Cellular MT2 accumulation upon neogenin depletion could result from an increase in *TMPRSS6* gene expression, a decrease in MT2 degradation, or both. Analysis of *Tmprss6* mRNA by qRT-PCR revealed no significant change either in the liver of neogenin mutant mice compared with wild type counterparts (Fig. 4*E*) or in HepG2 cells and HepG2-MT2 cells after depletion of neogenin (data not shown). The transcription of transfected *TMPRSS6* cDNA in HepG2-MT2 cells is under the control of a CMV promoter. These results suggest that the increased MT2 levels detected in neogenin mutant mice, as well as in HepG2-MT2 cells with neogenin knockdown, did not result from the increased transcription of *Tmprss6* gene or the increased stability of *Tmprss6* mRNA.

The effects of neogenin knockdown on MT2 degradation were tested. Cycloheximide at 100 μg/ml was added into the culture medium of HepG2-MT2 cells to block protein synthesis. Depletion of endogenous neogenin was able to significantly prevent the rapid decrease in MT2 (Fig. 5, *A* and *B*). These results indicate that the accumulation of MT2 upon neogenin knockdown results from the reduced MT2 degradation and indirectly imply that neogenin facilitates MT2 degradation.

To determine whether neogenin enhances MT2 degradation by mediating its internalization, we tested the effects of dynasore, a cell-permeable inhibitor specific for the dynamin GTPase (45), on cellular MT2 levels. A recent study indicates that cell surface MT2 undergoes internalization via a dynamin-dependent pathway and that the internalized MT2 is targeted to lysosomes for degradation (46). Incubation of HepG2-MT2 cells in the presence of 160 μM dynasore resulted in an accumulation of MT2 (Fig. 5*C*). The concentration of dynasore used was based on a previous study using HepG2 cells (29). This result implies that neogenin is

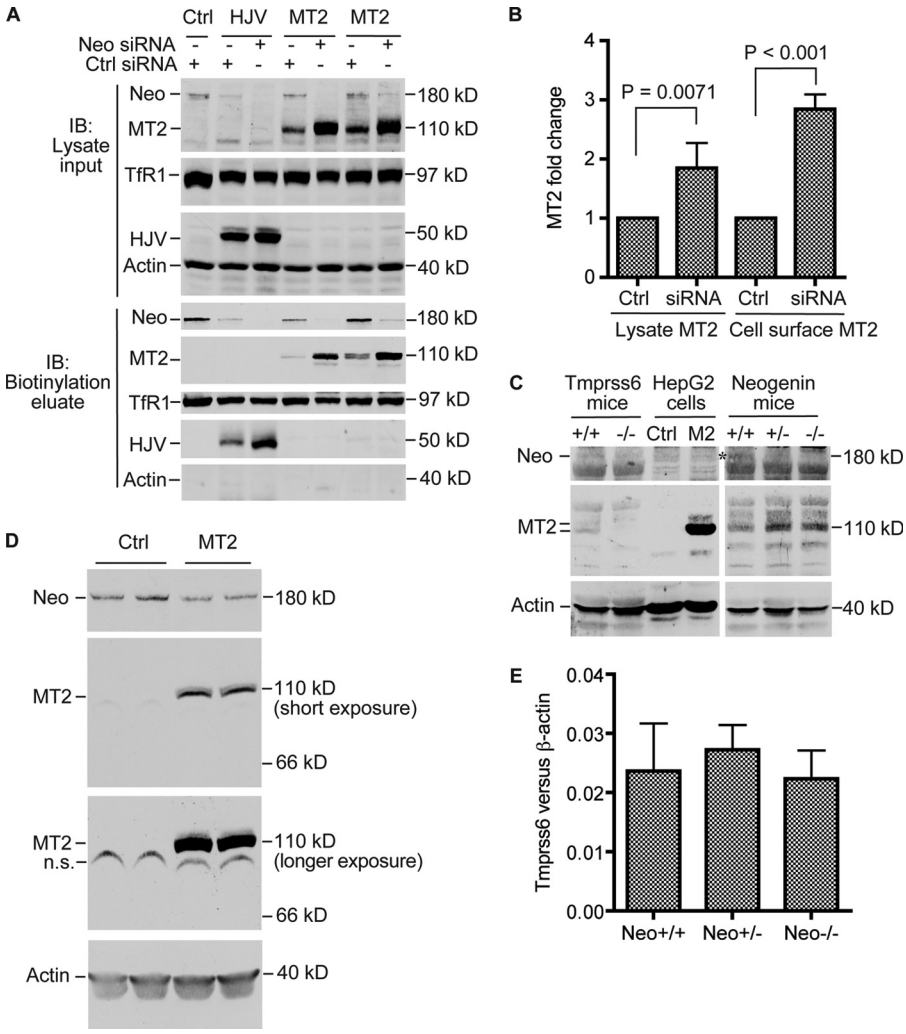

FIGURE 4. **Depletion of neogenin results in the accumulation of both cellular and cell surface MT2.** *A,* knockdown of endogenous neogenin increases the MT2 levels both in the cell extracts and on the plasma membrane. HepG2 cells stably expressing MT2 or HJV were transfected with a control or neogenin siRNA twice on day 1 and day 3. At about 72 h after the second transfection, cell surface proteins were biotinylated at 4 °C. The biotinylated proteins in the cell lysate were isolated using streptavidin-agarose beads. Neogenin, MT2, TfR1, HJV, and β-actin in about 10% of total cell lysate prior to pulldown (lysate input) and in the total eluates from streptavidin-agarose beads (biotinylation eluate) were immunoblotted (*IB*) using the corresponding antibodies. Two individual HepG2-MT2 clones were used for the analysis. Image in the *3rd panel* was obtained by a sequential probing with anti-HJV and β-actin antibodies. One antibody was applied each time. The membrane was not stripped before the following antibody was applied. The experiments were repeated four times with consistent results. *B,* quantification of the immunodetection for MT2 in *A*. MT2 bands as showed in *A* were quantified using an Alexa Fluor 680 goat anti-rabbit secondary antibody and an Odyssey Infrared Imaging System (Licor). The intensities of MT2 bands in cell lysate were normalized to that of the corresponding β-actin. The relative levels of MT2 in control (*Ctrl*) siRNA-transfected cells were counted as 1. Pair and two-tailed *t* test was used to calculate the difference of relative MT2 levels between control and neogenin siRNA transfection. Results are from four individual experiments. *C,* neogenin mutant mice have an increased MT2 level. About 250 μg of liver membrane proteins from age- and gender-matched wild type (+/+), heterozygous (+/−), or homozygous (−/−) neogenin mutant mice was subjected to SDS-PAGE and immunodetection of neogenin (*Neo*), MT2, and β-actin. Liver membrane extracts from a pair of age- and gender-matched wild type (+/+) and *Tmprss6*-null (−/−) mice and cell lysates from HepG2-Ctrl and MT2 (M2) lysates were included as controls. * indicates the neogenin band. The results were repeated twice in two different sets of neogenin mutant mice with consistent results. *D,* Western blot analysis of neogenin and MT2 in HepG2-Ctrl (*Ctrl*) and HepG2-MT2 cells (*MT2*). Two MT2 images (short exposure and longer exposure) were illustrated to show the lack of detectable autocleavage products of MT2. The experiments were repeated four times with consistent results. *n.s.* denotes the nonspecific band. *E,* quantitative RT-PCR analysis of *Tmprss6* mRNA expression in age and gender-matched wild type ($Neo^{+/+}$), heterozygous ($Neo^{+/-}$), or homozygous ($Neo^{-/-}$) neogenin mutant mice. There are five animals per group. The results are expressed as the amount of mRNA relative to β-actin in each sample. No significant difference was detected between groups.

required for the rapid turnover of MT2 through facilitating its internalization.

Similarly, incubation with the full-length soluble neogenin ectodomain led to an increase in MT2 (Fig. 5*D*). The soluble neogenin FNIII 5–6 domains but not the FNIII 1–6 domains also led to a barely detectable increase in MT2 (Fig. 5*D*). We speculate that soluble neogenin FNIII 1–6 domain may not be able to disrupt the neogenin-MT2 interactions. The relatively mild accumulation of MT2 in the presence of soluble neogenin ectodomain might result from the incomplete disruption of neogenin/MT2. The binding affinity between neogenin and MT2 has not been defined. Together, our observations suggest that neogenin enhances MT2 degradation by facilitating cell surface MT2 internalization in a dynamin-dependent manner.

We also explored the potential mechanism for the increase in cell surface HJV upon neogenin knockdown (Fig. 4*A*). Our previous studies imply that HJV is internalized in a dynamin-independent but cholesterol-dependent manner (29). Consistently, suppression of dynamin GTPase activity by dynasore only resulted in a mild accumulation of cellular HJV in HepG2-HJV cells (data not

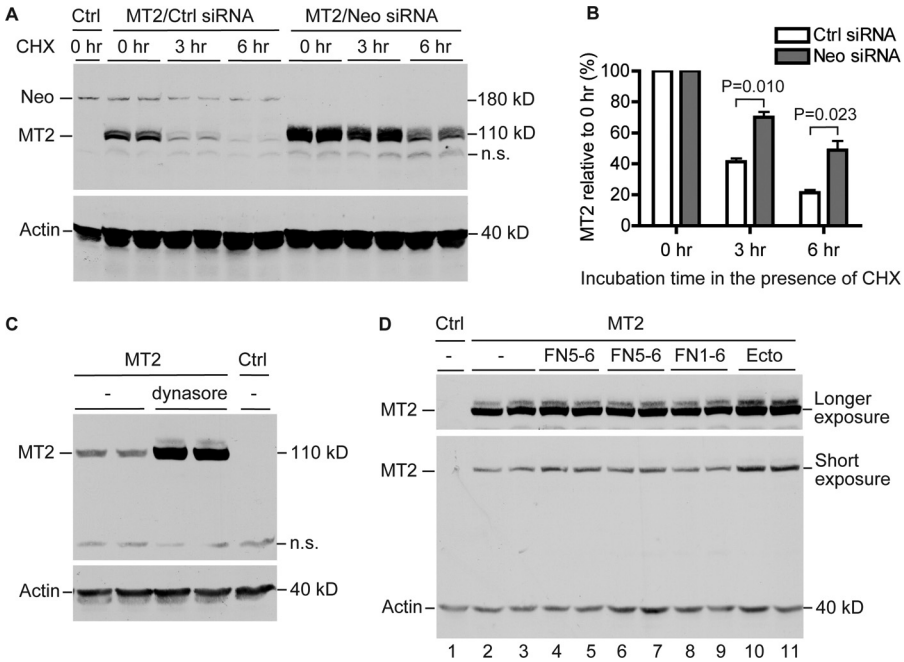

FIGURE 5. **Disruption of neogenin-MT2 interaction slows down MT2 degradation.** *A,* depletion of endogenous neogenin reduces MT2 degradation. HepG2-MT2 cells were transfected with a control (*Ctrl*) or neogenin siRNA twice on day 1 and day 3. At about 66 h after the second transfection, cells were incubated with 100 μg/ml cycloheximide (*CHX*) in complete medium for 0, 3, and 6 h. Cell lysates were then prepared and analyzed by immunoblotting using anti-neogenin (*Neo*), MT2, and β-actin (*Actin*) antibodies. HepG2 cells stably transfected with a pcDNA3.1 empty vector (*Ctrl*) were included as a negative control for MT2. *n.s.* denotes nonspecific band. *B,* quantification of the immunodetection for MT2 in *A*. MT2 bands as shown in *A* were quantified using an Alexa Fluor 680 goat anti-rabbit secondary antibody and an Odyssey Infrared Imaging System (Licor). The intensities of MT2 bands in cell lysate were normalized to that of the corresponding β-actin. The relative levels of MT2 at 3 and 6 h were then expressed as the percentage relative to 0 h for each group. Pair and two-tailed *t* tests were used to calculate the difference of relative MT2 levels between control and neogenin siRNA transfection. *Error bars* represent the standard deviation. Results are from four individual experiments. *C,* incubation with dynasore results in an accumulation of MT2 in HepG2-MT2 cells. HepG2-MT2 cells were incubated in complete medium with 160 μM dynasore (Sigma) in DMSO or an equal volume of DMSO (−) for 18 h. Cell lysates were prepared for immunodetection of MT2 and β-actin. The experiments were repeated three times with consistent results. *D,* incubation with soluble neogenin ectodomain results in a mild accumulation of MT2 in HepG2-MT2 cells. HepG2-MT2 cells were incubated with 40 nM neogenin FNIII 5–6 from two different preparations (*FN5–6*), 0.25 μM neogenin FNIII 1–6 (*FN1–6*), or 0.5 μM soluble neogenin ectodomain (*Ecto*) in DMEM, 5% FCS for 18 h. MT2 and β-actin in cell lysate were immunodetected. Two MT2 images (short exposure and longer exposure) were illustrated. The experiments were repeated three times with consistent results.

shown). Similar to MT2, incubation of HepG2-HJV cells with soluble neogenin ectodomain (~150 kDa) led to an evident accumulation of cellular HJV (Fig. 1*F*). These results suggest that neogenin also facilitates the internalization of cell surface HJV.

MT2 Traffics to the Plasma Membrane via the Traditional Biosynthetic Pathway—To explore the mechanism by which neogenin is involved in MT2 cleavage of HJV, we investigated the route of MT2 trafficking by analyzing the maturation of Asn-linked oligosaccharides on MT2, using Endo-H, which cleaves high mannose oligosaccharides added co-translationally in the ER, and PNGase F, which cleaves both high mannose and Golgi-modified (complex) oligosaccharides. MT2, neogenin, and HJV contain Asn-linked oligosaccharides (21, 31, 36). Our previous studies indicate that neogenin and HJV traffic from the ER to the plasma membrane possibly via different routes (36). Although neogenin follows the traditional biosynthetic pathway, the oligosaccharides on HJV avoid obtaining Golgi-specific modifications until HJV undergoes retrograde trafficking from the cell surface (36). The MT2 sequence possesses seven potential Asn-linked glycosylation sites (21). In this set of studies, biotinylated cell surface proteins after streptavidin bead pulldown were digested with either Endo-H or PNGase F. A decrease in the molecular weight of MT2, as detected by Western blot analysis, indicates the removal of oligosaccharides. Most of the cell surface MT2 was sensitive to PNGase F but not to Endo-H (Fig. 6*A, lane 2 versus lanes 3* and *4*). This indicates that MT2 obtained complex oligosaccharides during its transit through the Golgi. Consistent with our previous studies (36), the majority of endogenously expressed cell surface neogenin was Endo-H-resistant (Fig. 6*A*). As expected, Na^+/K^+-ATPase α1, a plasma membrane protein that possesses no potential Asn-linked glycosylation site in its sequence, remains unaffected by Endo-H or PNGase F digestion (Fig. 6*A*). Together, these results suggest that MT2 traffics through the traditional biosynthetic pathway, which is similar to neogenin but distinct from HJV. These observations imply that HJV is not accessible to MT2 for cleavage on the biosynthetic pathway.

MT2 Cleaves HJV after It Reaches the Cell Surface—We previously showed that both intracellular and cell surface HJV are sensitive to Endo-H digestion, but the secreted HJV is Endo-H-resistant (36). To determine the potential site where MT2 cleavage of HJV occurs, the secreted HJV in the media from HEK293-HJV/MT2 cells was subjected to Endo-H and PNGase F digestion, followed by detection of HJV by Western blot. Consistent with the observations by Silvestri *et al.* (21), expression of MT2 resulted in a decrease in cellular HJV (Fig. 6*B, upper panel, lane 2 versus 5*). Interestingly, the secreted HJV by both MT2 cleavage (Fig. 6*B, lanes 12–14*) and furin cleavage (Fig. 6*B, lanes 9–11*) was resistant to Endo-H but sensitive to PNGase F,

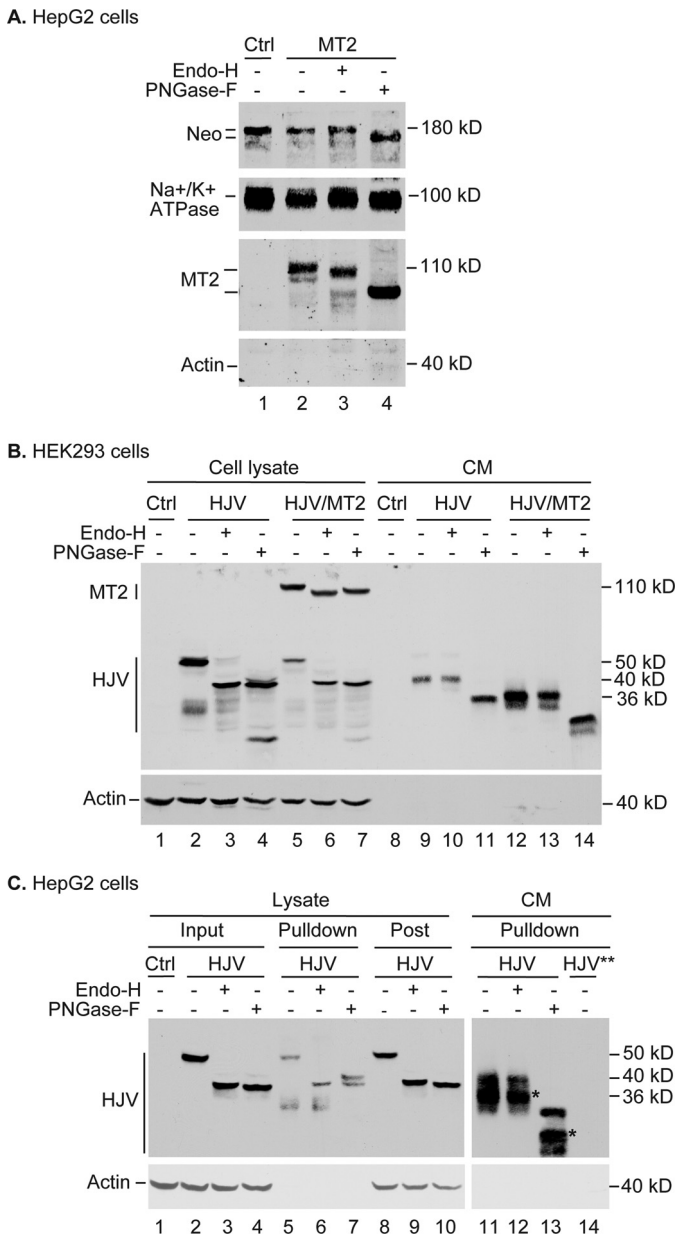

FIGURE 6. **MT2 and HJV traffic to the plasma membrane through distinct pathways.** *A,* MT2 traffics to the plasma membrane through the traditional biosynthetic pathway. Cell surface proteins in HepG2-MT2 cells were biotinylated at 4 °C. The biotinylated proteins in the cell lysate were isolated using streptavidin-agarose beads. Bound proteins were eluted with NET-Triton, 1% β-mercaptoethanol, 0.5% SDS. The eluates were subjected to digestion with mock, Endo-H, or PNGase F, followed by immunodetection of neogenin (*Neo*), Na^+/K^+-ATPase α1 (a specific plasma membrane marker), MT2, and β-actin. All images are from a single gel. The experiment was repeated four times with consistent results. *Ctrl*, control. *B,* MT2-cleaved soluble HJV is resistant to Endo-H digestion in HEK293 cells. HEK293-HJV cells in a 12-well plate were transiently transfected with either pcDNA3 empty vector (*HJV*) or MT2 cDNA (*HJV/MT2*). At 48 h post-transfection, culture medium was changed to DMEM, 1% FCS. After 16 h of incubation, CM was collected, and cell lysate was prepared. One-third of cell lysate and ~15% of CM were subjected to mock, Endo-H, and PNGase F digestion, followed by SDS-PAGE separation and immunodetection of MT2, HJV, and β-actin. The image is a representative of four independent experiments with consistent results. *C,* cell surface HJV has high mannose oligosaccharides, whereas MT2-cleaved cell surface HJV has complex oligosaccharides in HepG2 cells. Cell surface HJV in HepG2-HJV cells was biotinylated at 4 °C, followed by incubation at 37 °C for 4 h in complete medium. The total biotinylated HJV in cell lysate (*Lysate/Pulldown*) and the biotinylated HJV released into the medium (*CM/Pulldown*) were isolated using streptavidin-agarose beads. The eluates were digested with Endo-H and PNGase F. Endo-H and PNGase F digestion of one-third of input cell lysates (*Lysate/Input*) and one-third of cell lysate after streptavidin pulldown (*Lysate/Post*) are also included. Lysate from HepG2-Ctrl cells (*Lysate/Input/Ctrl*) or pulldown from the medium of HepG2-HJV cells without biotinylation (*CM/Pulldown/HJV***) were used as negative controls. * indicates the MT2-cleaved HJV products in the CM. Experiments were repeated four times with consistent results.

indicating that they acquired complex oligosaccharides before release.

Our previous studies suggest that cleavage of HJV takes place after it traffics to the plasma membrane (29). To gain more insight into the cleavage of HJV by MT2, we followed the transition of Asn-linked oligosaccharides of HJV labeled at the cell surface from high mannose to complex forms. HepG2 cells were used because they express a low level of TMPRSS6 (20), which cleaves HJV (Fig. 1, *C* and *E*). The secretion of biotinylated cell surface HJV was measured 4 h after warming the cells to 37 °C. Both the total biotinylated cell surface HJV and the secreted HJV were isolated using streptavidin beads. As predicted, two major secreted forms of soluble HJV were detected that migrate at 36 kDa (MT2 cleavage product) and 40 kDa (furin cleavage product) in SDS-PAGE, respectively (Fig. 6*C, lane 11*). Both cleaved forms of HJV in the conditioned medium were sensitive to PNGase but not Endo-H indicating that HJV had undergone a conversion from a high-mannose to a complex oligosaccharide form prior to release into the medium. Interestingly, the secretion of cell surface HJV was correlated with a transition from Endo-H-sensitive to Endo-H-resistant (Fig. 6*C, lane 6 versus 12*), which is consistent with the observations in HEK293 cells (Fig. 6*B*) and our previous studies (36). These results suggest that both MT2- and furin-mediated release of HJV from HepG2 cells involves a retrograde trafficking of cell surface HJV possessing high mannose oligosaccharides to the TGN and Golgi, where its oligosaccharides are processed to a complex form. However, these observations are unable to distinguish whether cleavage occurs at the cell surface prior to endocytosis, processing, and release or in endocytic or recycling vesicles.

DISCUSSION

MT2 regulates iron homeostasis by cleaving membrane-bound HJV in hepatocytes (20, 21, 23, 24). In this study we showed that neogenin forms a complex with both MT2 and HJV. Disruption of neogenin-HJV interaction at the cell surface abolishes MT2 cleavage of HJV. MT2 traffics to the plasma membrane through the traditional biosynthetic pathway independently of neogenin. HJV cleavage by MT2 takes place after it reaches the plasma membrane, and the cleaved HJV products undergo a post-translational modification in the TGN/Golgi compartments before being secreted from the cells.

Hepatocyte HJV acts as a co-receptor for BMP ligands to induce hepcidin expression via the BMP/Smad signaling pathway (11). Lack of functional HJV in humans (5) or loss of Hjv specifically in murine hepatocytes (14, 15) markedly reduces hepatic hepcidin expression and results in severe iron overload. HJV is regulated at the protein level by MT2 and possibly furin. MT2 is a serine protease that is co-expressed with HJV in hepatocytes (16–18). It binds to and cleaves membrane-bound HJV into the inactive form (20, 21), which leads to the decrease in

the level of cellular HJV (21) as well as the reduction of HJV-induced hepcidin expression (18, 21). Consistently, the lack of functional MT2 in humans and mice results in increased hepcidin expression and iron deficiency (6, 18, 22). Interestingly, the function of MT2 could not be compensated for by the ubiquitously expressed furin (27), which also cleaves HJV but at a distinct site from MT2 (20). Thus, MT2 is the key suppressor of hepcidin expression.

HJV binds neogenin (7, 33), a ubiquitously expressed multifunctional transmembrane protein. It is also a receptor for RGMa, netrins, and possibly BMP ligands (32, 48–50). This study demonstrated that neogenin-HJV interaction is the prerequisite for HJV cleavage by both MT2 and furin. These are consistent with our previous observations in HepG2 and C2C12 cells (28, 29). Our previous studies suggest that MT2 cleaves HJV independently of furin (20). Neogenin could be required for the cleavage of HJV by MT2 and/or the subsequent secretion of cleaved product. Because no accumulation of cleaved HJV was detected within the cell extracts upon neogenin knockdown, neogenin appears to facilitate MT2 cleavage of HJV, in addition to furin.

Neogenin binds to HJV through its FNIII 5–6 domains (34). We examined the effects of three soluble forms of neogenin (FNIII 5–6, FNIII 1–6, and Neo/Ecto) that could bind HJV *in vitro*, on MT2 cleavage of HJV. These are predicted to competitively disrupt the interaction of HJV with the endogenous full-length neogenin at the plasma membrane. All three forms of neogenin blocked MT2 cleavage of HJV, implying that MT2 could only cleave the HJV that is associated with the full-length neogenin. Because neogenin FNIII 5–6 domains are located immediately adjacent to the transmembrane (Fig. 1*B*), association of HJV with neogenin at the plasma membrane may result in a pronounced conformational change of HJV. We hypothesize that this change would lead to the exposure of the MT2 cleavage site in HJV.

MT2 binds HJV through its stem region (21). Here, we showed that MT2 also interacts with neogenin and that HJV could form a complex with both MT2 and neogenin, but MT2 does not cleave neogenin. MT2 is predicted to cleave substrate at arginine residues (16). These observations support the idea that HJV is a specific substrate of MT2. Hepatocytes are the only known cell type where MT2, HJV, and neogenin are co-expressed (17, 35). This would allow neogenin to facilitate MT2 cleavage of HJV.

MT2 cleaves HJV by its C-terminal catalytic domain. Lack of this domain in *mask* mice or disruption of both *Tmprss6* alleles in mice results in a marked increase in hepatic hepcidin expression as well as microcytic anemia (16, 22, 24). However, the precise active form of MT2 is still debatable. One study suggests that the full-length MT2 is catalytically inactive zymogen (21). Activation of MT2 requires the cleavage of the catalytic domain at the predicted autocleavage site at the plasma membrane, and the cleaved catalytic domain forms a heterodimer with the stem region of MT2 through disulfide bonds (21). Other groups report that only the shed MT2 catalytic domain from the cells is enzymatically active because it cleaves the synthetic peptide (51). Our results favor the former. In HEK293 cells that were transiently expressing MT2 with a *myc* tag at the end of catalytic domain, we detected the shed MT2 catalytic domain in the conditioned medium (data not shown). Addition of a *myc* tag does not affect the catalytic activity of MT2 (18), but co-culture studies suggest that only the cell-associated MT2 is able to cleave HJV (18). In this study, no cleaved form of MT2 was detected in HepG2-MT2 cells by immunoprecipitation using an antibody against the stem region of MT2 or by Western blot analysis of biotinylated cell surface MT2. Yet these observations do not exclude the possibilities that only a small proportion of MT2 exists as an active form at the cell surface. Its level may fall below the limit of detection. For example, HepG2 cells express an undetectable amount of MT2 by Western blot analysis, but the endogenous MT2 is sufficient to cleave HJV.

The finding that down-regulation of neogenin increases (rather than decreases) MT2 on the cell surface is an unexpected observation. Studies by Beliveau *et al.* (46) indicate that cell surface MT2 is internalized via a dynamin-dependent pathway and that the internalized MT2 is targeted to lysosomes for degradation. In line with this previous finding, we provide evidence showing that depletion of neogenin reduces the rate of MT2 degradation and that inhibition of endocytosis results in an accumulation of MT2 in the cells. On the basis of these results, we predict that neogenin facilitates MT2 internalization to mediate its rapid degradation.

This and our previous studies (28) indicate that HJV traffics to the cell surface independently of neogenin. When endogenous neogenin is depleted, increases of both MT2 and HJV at the cell surface are unable to trigger MT2 cleavage of HJV. We speculate that the functional form of MT2 exists at least as a hetero-oligomer with neogenin. MT2 may act like the γ-secretase, a heterotetramer that contains at least presenilin 1, nicastrin, Aph-1, and Pen2. In this complex, presenilin1 is the only component that cleaves the amyloid precursor protein (51). Alternatively, interaction with neogenin may elicit the autocleavage of MT2 catalytic domain that leads to the activation of MT2, and the cleaved products are rapidly degraded.

HJV is predicted to traffic to the plasma membrane avoiding the Golgi processing either by being masked by binding to another protein or by bypassing the Golgi (36). Both neogenin and MT2 appear to traffic to the plasma membrane through the traditional biosynthetic pathway in HepG2 cells as measured by the gain of complex oligosaccharides. These observations have two important implications. First, distinct trafficking pathways of HJV, neogenin, and MT2 would prevent the exposure of HJV to MT2 on the biosynthetic pathway. Importantly, this would allow the specific regulation of HJV levels by MT2 at the plasma membrane through the body iron sensory machinery. Although HJV mRNA expression is not regulated by iron, the MT2 protein seems to be stabilized in rats with an acute iron deficiency (17), and MT2 mRNA expression is induced via BMP signaling through a feedback mechanism (38). Second, neogenin and MT2 trafficking through the same pathways would allow neogenin to facilitate the function of MT2 presumably by forming a heterodimer. The findings that only a very small proportion of MT2 was detected at the plasma membrane in this study might be due to the fact that an overexpression system was used for the analysis. Transfected MT2 undergoes a rapid turnover (17). Our previous studies showed that the transfected MT2 in

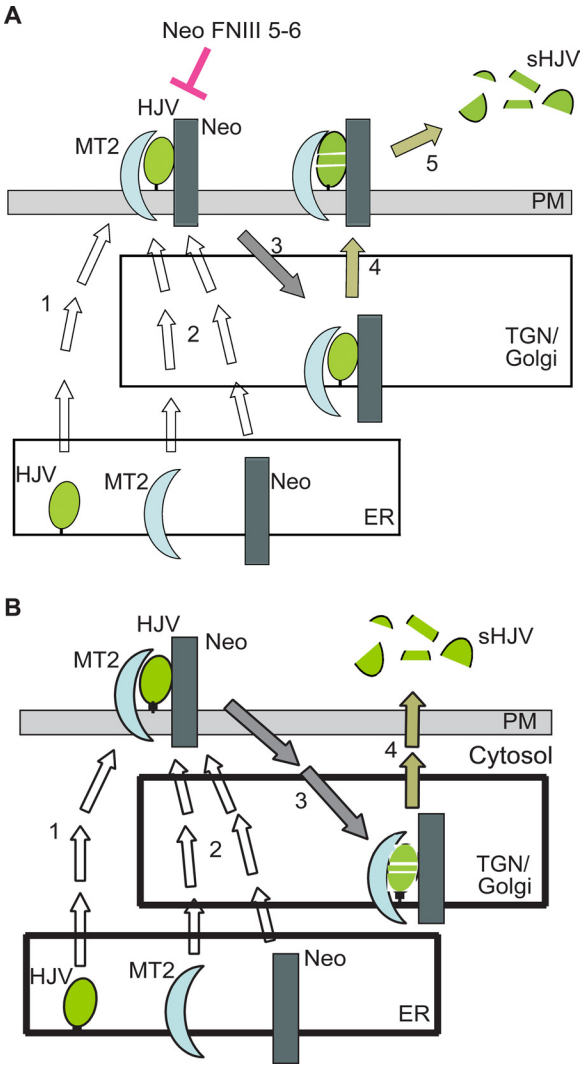

FIGURE 7. **Models of HJV, MT2, and neogenin trafficking in hepatocytes.** *A,* model of MT2 cleavage of HJV at the plasma membrane after retrograde transport. Nascent HJV traffics from ER to plasma membrane bypassing the Golgi compartment (*1*), and MT2 and neogenin follow the traditional biosynthetic pathway and undergo post-translational modifications in the TGN/Golgi compartment (*2*). Upon reaching the plasma membrane, HJV forms a complex with MT2 and neogenin, which triggers the internalization and retrograde trafficking of the complex into the TGN/Golgi compartment for post-translational modifications of HJV (*3*). Then the complex traffics back to the plasma membrane (*4*) to allow MT2 cleavage of HJV. The cleaved HJV is released from the cells (*5*). *B,* model of MT2 cleavage of HJV during retrograde transport. Nascent HJV, MT2, and neogenin traffic from ER to plasma membrane as described in *A* (*1* and *2*). Upon reaching the plasma membrane, HJV forms a complex with MT2 and neogenin, which triggers the internalization and retrograde trafficking of the complex into the TGN/Golgi compartment for cleavage (*3*). The cleaved HJV by MT2 in this compartment is rapidly secreted from the cells (*4*).

HepG2 cells is able to cleave HJV, and therefore it is functional (20). To the best of our knowledge, the relative ratios of cell surface to intracellular MT2 (or HJV) *in vivo* have not been reported. Immunofluorescent studies did show a significant amount of HJV localized within HepG2-HJV cells (data not shown).

Studies by others assume that MT2 cleaves HJV at the plasma membrane (21, 39). Consistently, we found that MT2 does not cleave HJV in the biosynthetic pathway. We also provide evidence showing that both MT2 and furin-mediated HJV cleavage are coupled to a transition of Asn-linked oligosaccharides from high mannose to complex oligosaccharides in HJV. Although cell surface HJV possesses high mannose oligosaccharides, the secreted HJV products gain complex oligosaccharides. Glycoproteins are processed to the complex oligosaccharides only in the TGN and Golgi (52). However, our results do not exclude the possibility that MT2 cleaves HJV at the plasma membrane. Dissociation from neogenin might require a retrograde trafficking though an acidic compartment.

On the basis of the published data and the results in this study, we propose two models for MT2 trafficking and cleavage of HJV in hepatocytes (Fig. 7, *A* and *B*). Nascent MT2 traffics from the ER to the plasma membrane via the Golgi/TGN in a manner similar to neogenin. Upon reaching the cell surface, HJV forms a ternary complex with both neogenin and MT2, which undergoes endocytosis and retrograde trafficking to the Golgi/TGN compartments for further modification before recycling to the plasma membrane where it is cleaved by MT2 and then released (Fig. 7*A*). Alternatively cleavage occurs in endocytic compartments (Fig. 7*B*).

Neogenin mutant mice have multiple defects, in addition to defects of iron metabolism (44, 53). This might be due to the fact that neogenin is also a receptor for several other ligands (32, 47, 50). The severe iron overload and marked decrease in hepatic hepcidin expression detected in the homozygous mutant mice are similar to the phenotype of *Hjv*-null mice (44). This is consistent with our findings showing that neogenin is essential for BMP4-induced and HJV-mediated hepcidin expression in HepG2 cells (35). Based on these previous observations and findings in this study, we hypothesize that neogenin modulates the function of HJV through at least the following two pathways to foster the HJV-induced BMP signaling and to mediate the MT2 cleavage of HJV. The defects of iron homeostasis in neogenin mutant mice appear to result from the blunted BMP signaling. How neogenin coordinately mediates these two processes *in vivo* is the subject of our future studies.

Acknowledgments—We thank Dr. Fan Yang and Dr. Pamela Bjorkman, California Institute of Technology, for the purified soluble neogenin preparations; Dr. Thomas Bartnikas and Dr. Mark Fleming, Harvard University, for Tmprss6$^{-/-}$ mice liver tissues; and Ningning Zhao and Juxing Chen for critical reading of this manuscript and helpful comments.

REFERENCES

1. Ganz, T., and Nemeth, E. (2011) Hepcidin and disorders of iron metabolism. *Annu. Rev. Med.* **62,** 347–360
2. De Domenico, I., McVey Ward, D., and Kaplan, J. (2008) Regulation of iron acquisition and storage. Consequences for iron-linked disorders. *Nat. Rev. Mol. Cell Biol.* **9,** 72–81
3. Roetto, A., Papanikolaou, G., Politou, M., Alberti, F., Girelli, D., Christakis, J., Loukopoulos, D., and Camaschella, C. (2003) Mutant antimicrobial peptide hepcidin is associated with severe juvenile hemochromatosis. *Nat. Genet.* **33,** 21–22
4. Weinstein, D. A., Roy, C. N., Fleming, M. D., Loda, M. F., Wolfsdorf, J. I., and Andrews, N. C. (2002) Inappropriate expression of hepcidin is associated with iron refractory anemia. Implications for the anemia of chronic disease. *Blood* **100,** 3776–3781
5. Papanikolaou, G., Samuels, M. E., Ludwig, E. H., MacDonald, M. L., Franchini, P. L., Dubé, M. P., Andres, L., MacFarlane, J., Sakellaropoulos,

N., Politou, M., Nemeth, E., Thompson, J., Risler, J. K., Zaborowska, C., Babakaiff, R., Radomski, C. C., Pape, T. D., Davidas, O., Christakis, J., Brissot, P., Lockitch, G., Ganz, T., Hayden, M. R., and Goldberg, Y. P. (2004) Mutations in HFE2 cause iron overload in chromosome 1q-linked juvenile hemochromatosis. *Nat. Genet.* **36,** 77–82

6. Finberg, K. E., Heeney, M. M., Campagna, D. R., Aydinok, Y., Pearson, H. A., Hartman, K. R., Mayo, M. M., Samuel, S. M., Strouse, J. J., Markianos, K., Andrews, N. C., and Fleming, M. D. (2008) Mutations in TMPRSS6 cause iron-refractory iron deficiency anemia (IRIDA). *Nat. Genet.* **40,** 569–571
7. Zhang, A. S., West, A. P., Jr., Wyman, A. E., Bjorkman, P. J., and Enns, C. A. (2005) Interaction of hemojuvelin with neogenin results in iron accumulation in human embryonic kidney 293 cells. *J. Biol. Chem.* **280,** 33885–33894
8. Lanzara, C., Roetto, A., Daraio, F., Rivard, S., Ficarella, R., Simard, H., Cox, T. M., Cazzola, M., Piperno, A., Gimenez-Roqueplo, A. P., Grammatico, P., Volinia, S., Gasparini, P., and Camaschella, C. (2004) Spectrum of hemojuvelin gene mutations in 1q-linked juvenile hemochromatosis. *Blood* **103,** 4317–4321
9. Huang, F. W., Pinkus, J. L., Pinkus, G. S., Fleming, M. D., and Andrews, N. C. (2005) A mouse model of juvenile hemochromatosis. *J. Clin. Invest.* **115,** 2187–2191
10. Niederkofler, V., Salie, R., and Arber, S. (2005) Hemojuvelin is essential for dietary iron sensing, and its mutation leads to severe iron overload. *J. Clin. Invest.* **115,** 2180–2186
11. Babitt, J. L., Huang, F. W., Wrighting, D. M., Xia, Y., Sidis, Y., Samad, T. A., Campagna, J. A., Chung, R. T., Schneyer, A. L., Woolf, C. J., Andrews, N. C., and Lin, H. Y. (2006) Bone morphogenetic protein signaling by hemojuvelin regulates hepcidin expression. *Nat. Genet.* **38,** 531–539
12. Xia, Y., Babitt, J. L., Sidis, Y., Chung, R. T., and Lin, H. Y. (2008) Hemojuvelin regulates hepcidin expression via a selective subset of BMP ligands and receptors independently of neogenin. *Blood* **111,** 5195–5204
13. Zhang, A. S., Gao, J., Koeberl, D. D., and Enns, C. A. (2010) The role of hepatocyte hemojuvelin in the regulation of bone morphogenic protein-6 and hepcidin expression *in vivo*. *J. Biol. Chem.* **285,** 16416–16423
14. Chen, W., Huang, F. W., de Renshaw, T. B., and Andrews, N. C. (2011) Skeletal muscle hemojuvelin is dispensable for systemic iron homeostasis. *Blood* **117,** 6319–6325
15. Gkouvatsos, K., Wagner, J., Papanikolaou, G., Sebastiani, G., and Pantopoulos, K. (2011) Conditional disruption of mouse *HFE2* gene. Maintenance of systemic iron homeostasis requires hepatic but not skeletal muscle hemojuvelin. *Hepatology* **54,** 1800–1807
16. Velasco, G., Cal, S., Quesada, V., Sánchez, L. M., and López-Otín, C. (2002) Matriptase-2, a membrane-bound mosaic serine proteinase predominantly expressed in human liver and showing degrading activity against extracellular matrix proteins. *J. Biol. Chem.* **277,** 37637–37646
17. Zhang, A. S., Anderson, S. A., Wang, J., Yang, F., DeMaster, K., Ahmed, R., Nizzi, C. P., Eisenstein, R. S., Tsukamoto, H., and Enns, C. A. (2011) Suppression of hepatic hepcidin expression in response to acute iron deprivation is associated with an increase of matriptase-2 protein. *Blood* **117,** 1687–1699
18. Du, X., She, E., Gelbart, T., Truksa, J., Lee, P., Xia, Y., Khovananth, K., Mudd, S., Mann, N., Moresco, E. M., Beutler, E., and Beutler, B. (2008) The serine protease TMPRSS6 is required to sense iron deficiency. *Science* **320,** 1088–1092
19. Ramsay, A. J., Hooper, J. D., Folgueras, A. R., Velasco, G., and López-Otín, C. (2009) Matriptase-2 (TMPRSS6). A proteolytic regulator of iron homeostasis. *Haematologica* **94,** 840–849
20. Maxson, J. E., Chen, J., Enns, C. A., and Zhang, A. S. (2010) Matriptase-2- and proprotein convertase-cleaved forms of hemojuvelin have different roles in the down-regulation of hepcidin expression. *J. Biol. Chem.* **285,** 39021–39028
21. Silvestri, L., Pagani, A., Nai, A., De Domenico, I., Kaplan, J., and Camaschella, C. (2008) The serine protease matriptase-2 (TMPRSS6) inhibits hepcidin activation by cleaving membrane hemojuvelin. *Cell Metab* **8,** 502–511
22. Folgueras, A. R., de Lara, F. M., Pendás, A. M., Garabaya, C., Rodríguez, F., Astudillo, A., Bernal, T., Cabanillas, R., López-Otín, C., and Velasco, G. (2008) Membrane-bound serine protease matriptase-2 (Tmprss6) is an essential regulator of iron homeostasis. *Blood* **112,** 2539–2545
23. Truksa, J., Gelbart, T., Peng, H., Beutler, E., Beutler, B., and Lee, P. (2009) Suppression of the hepcidin-encoding gene *Hamp* permits iron overload in mice lacking both hemojuvelin and matriptase-2/TMPRSS6. *Br. J. Haematol.* **147,** 571–581
24. Finberg, K. E., Whittlesey, R. L., Fleming, M. D., and Andrews, N. C. (2010) Down-regulation of Bmp/Smad signaling by Tmprss6 is required for maintenance of systemic iron homeostasis. *Blood* **115,** 3817–3826
25. Lin, L., Nemeth, E., Goodnough, J. B., Thapa, D. R., Gabayan, V., and Ganz, T. (2008) Soluble hemojuvelin is released by proprotein convertase-mediated cleavage at a conserved polybasic RNRR site. *Blood Cells Mol Dis* **40,** 122–131
26. Silvestri, L., Pagani, A., and Camaschella, C. (2008) Furin-mediated release of soluble hemojuvelin. A new link between hypoxia and iron homeostasis. *Blood* **111,** 924–931
27. Thomas, G. (2002) Furin at the cutting edge. From protein traffic to embryogenesis and disease. *Nat. Rev. Mol. Cell Biol.* **3,** 753–766
28. Zhang, A. S., Anderson, S. A., Meyers, K. R., Hernandez, C., Eisenstein, R. S., and Enns, C. A. (2007) Evidence that inhibition of hemojuvelin shedding in response to iron is mediated through neogenin. *J. Biol. Chem.* **282,** 12547–12556
29. Zhang, A. S., Yang, F., Meyer, K., Hernandez, C., Chapman-Arvedson, T., Bjorkman, P. J., and Enns, C. A. (2008) Neogenin-mediated hemojuvelin shedding occurs after hemojuvelin traffics to the plasma membrane. *J. Biol. Chem.* **283,** 17494–17502
30. Lee, D. H., Lee, D. H., Zhou, L. J., Zhou, L. J., Zhou, Z., Xie, J. X., Xie, J. X., Jung, J. U., Liu, Y., Xi, C. X., Mei, L., and Xiong, W. C. (2010) Neogenin inhibits HJV secretion and regulates BMP-induced hepcidin expression and iron homeostasis. *Blood* **115,** 3136–3145
31. Meyerhardt, J. A., Look, A. T., Bigner, S. H., and Fearon, E. R. (1997) Identification and characterization of neogenin, a DCC-related gene. *Oncogene* **14,** 1129–1136
32. Matsunaga, E., Tauszig-Delamasure, S., Monnier, P. P., Mueller, B. K., Strittmatter, S. M., Mehlen, P., and Chédotal, A. (2004) RGM and its receptor neogenin regulate neuronal survival. *Nat. Cell Biol.* **6,** 749–755
33. Kuns-Hashimoto, R., Kuninger, D., Nili, M., and Rotwein, P. (2008) Selective binding of RGMc/hemojuvelin, a key protein in systemic iron metabolism, to BMP-2 and neogenin. *Am. J. Physiol. Cell Physiol* **294,** C994–C1003
34. Yang, F., West, A. P., Jr., Allendorph, G. P., Choe, S., and Bjorkman, P. J. (2008) Neogenin interacts with hemojuvelin through its two membrane-proximal fibronectin type III domains. *Biochemistry* **47,** 4237–4245
35. Zhang, A. S., Yang, F., Wang, J., Tsukamoto, H., and Enns, C. A. (2009) Hemojuvelin-neogenin interaction is required for bone morphogenic protein-4-induced hepcidin expression. *J. Biol. Chem.* **284,** 22580–22589
36. Maxson, J. E., Enns, C. A., and Zhang, A. S. (2009) Processing of hemojuvelin requires retrograde trafficking to the Golgi in HepG2 cells. *Blood* **113,** 1786–1793
37. Zhang, A. S., Xiong, S., Tsukamoto, H., and Enns, C. A. (2004) Localization of iron metabolism-related mRNAs in rat liver indicate that HFE is expressed predominantly in hepatocytes. *Blood* **103,** 1509–1514
38. Meynard, D., Vaja, V., Sun, C. C., Corradini, E., Chen, S., López-Otín, C., Grgurevic, L., Hong, C. C., Stirnberg, M., Gütschow, M., Vukicevic, S., Babitt, J. L., and Lin, H. Y. (2011) Regulation of TMPRSS6 by BMP6 and iron in human cells and mice. *Blood* **118,** 747–756
39. Babitt, J. L., and Lin, H. Y. (2011) The molecular pathogenesis of hereditary hemochromatosis. *Semin Liver Dis.* **31,** 280–292
40. Kuninger, D., Kuns-Hashimoto, R., Kuzmickas, R., and Rotwein, P. (2006) Complex biosynthesis of the muscle-enriched iron regulator RGMc. *J. Cell Sci.* **119,** 3273–3283
41. Okamura, Y., Kohmura, E., and Yamashita, T. (2011) TACE cleaves neogenin to desensitize cortical neurons to the repulsive guidance molecule. *Neurosci. Res.* **71,** 63–70
42. Leighton, P. A., Mitchell, K. J., Goodrich, L. V., Lu, X., Pinson, K., Scherz, P., Skarnes, W. C., and Tessier-Lavigne, M. (2001) Defining brain wiring patterns and mechanisms through gene trapping in mice. *Nature* **410,** 174–179

43. Mitchell, K. J., Pinson, K. I., Kelly, O. G., Brennan, J., Zupicich, J., Scherz, P., Leighton, P. A., Goodrich, L. V., Lu, X., Avery, B. J., Tate, P., Dill, K., Pangilinan, E., Wakenight, P., Tessier-Lavigne, M., and Skarnes, W. C. (2001) Functional analysis of secreted and transmembrane proteins critical to mouse development. *Nat. Genet.* **28,** 241–249
44. Zhou, Z., Xie, J., Lee, D., Liu, Y., Jung, J., Zhou, L., Xiong, S., Mei, L., and Xiong, W. C. (2010) Neogenin regulation of BMP-induced canonical Smad signaling and endochondral bone formation. *Dev. Cell* **19,** 90–102
45. Macia, E., Ehrlich, M., Massol, R., Boucrot, E., Brunner, C., and Kirchhausen, T. (2006) Dynasore, a cell-permeable inhibitor of dynamin. *Dev. Cell* **10,** 839–850
46. Béliveau, F., Brulé, C., Désilets, A., Zimmerman, B., Laporte, S. A., Lavoie, C. L., and Leduc, R. (2011) Essential role of endocytosis of the type II transmembrane serine protease TMPRSS6 in regulating its functionality. *J. Biol. Chem.* **286,** 29035–29043
47. Mawdsley, D. J., Cooper, H. M., Hogan, B. M., Cody, S. H., Lieschke, G. J., and Heath, J. K. (2004) The Netrin receptor neogenin is required for neural tube formation and somitogenesis in zebrafish. *Dev. Biol.* **269,** 302–315
48. Srinivasan, K., Strickland, P., Valdes, A., Shin, G. C., and Hinck, L. (2003) Netrin-1/neogenin interaction stabilizes multipotent progenitor cap cells during mammary gland morphogenesis. *Dev. Cell* **4,** 371–382
49. Rajagopalan, S., Deitinghoff, L., Davis, D., Conrad, S., Skutella, T., Chedotal, A., Mueller, B. K., and Strittmatter, S. M. (2004) Neogenin mediates the action of repulsive guidance molecule. *Nat. Cell Biol.* **6,** 756–762
50. Hagihara, M., Endo, M., Hata, K., Higuchi, C., Takaoka, K., Yoshikawa, H., and Yamashita, T. (2011) Palmitoylation controls dopamine transporter kinetics, degradation, and protein kinase C-dependent regulation. *J. Biol. Chem.* **286,** 5157–5165
51. De Strooper, B., and Annaert, W. (2010) Novel research horizons for presenilins and γ-secretases in cell biology and disease. *Annu. Rev. Cell Dev. Biol.* **26,** 235–260
52. Dennis, J. W., Nabi, I. R., and Demetriou, M. (2009) Metabolism, cell surface organization, and disease. *Cell* **139,** 1229–1241
53. Bae, G. U., Yang, Y. J., Jiang, G., Hong, M., Lee, H. J., Tessier-Lavigne, M., Kang, J. S., and Krauss, R. S. (2009) Neogenin regulates skeletal myofiber size and focal adhesion kinase and extracellular signal-regulated kinase activities *in vivo* and *in vitro*. *Mol. Biol. Cell* **20,** 4920–4931